AMERICAN SOCIETY FOR MICROBIOLOGY | Journal of Virology®

VIRUS-CELL INTERACTIONS

Role of Autophagy in HIV-1 Matrix Protein p17-Driven Lymphangiogenesis

Pietro Mazzuca,[a] Stefania Marsico,[b] Kai Schulze,[c] Stefania Mitola,[a] Marina C. Pils,[c] Cinzia Giagulli,[a] Carlos A. Guzman,[c] Arnaldo Caruso,[a] Francesca Caccuri[a]

Department of Molecular and Translational Medicine, University of Brescia Medical School, Brescia, Italy[a]; Department of Pharmacy, Health and Nutritional Sciences, University of Calabria, Arcavacata di Rende, Cosenza, Italy[b]; Helmholtz Centre for Infection Research, Braunschweig, Germany[c]

ABSTRACT AIDS-related lymphomas (ARLs) are expected to increase in the future since combined antiretroviral therapy (cART) enhances the life expectancy of HIV-1-infected (HIV$^+$) patients but does not affect the occurrence of ARLs to the same extent as that of other tumors. Lymphangiogenesis is essential in supporting growth and metastatic spreading of ARLs. HIV-1 does not infect the neoplastic B cells, but HIV-1 proteins have been hypothesized to play a key role in sustaining a prolymphangiogenic microenvironment in lymphoid organs. The HIV-1 matrix protein p17 is detected in blood and accumulates in the germinal centers of lymph nodes of HIV$^+$ patients under successful cART. The viral protein displays potent lymphangiogenic activity *in vitro* and *in vivo*. This is, at least in part, mediated by the secretion of the lymphangiogenic factor endothelin-1, suggesting that activation of a secretory pathway sustains the lymphangiogenic activity of p17. Here, we show that the p17 lymphangiogenic activity occurs on human lymph node-derived lymphatic endothelial cells (LN-LECs) under stress conditions only and relies entirely on activation of an autophagy-based pathway. In fact, induction of autophagy by p17 promotes lymphangiogenesis, whereas pharmacological and genetic inhibition of autophagy inhibits p17-triggered lymphangiogenesis. Similarly, the vasculogenic activity of p17 was totally inhibited in autophagy-incompetent mice. Our findings reveal a previously unrecognized role of autophagy in lymphangiogenesis and open the way to identify novel treatment strategies aimed at inhibiting aberrant tumor-driven lymphangiogenesis in HIV$^+$ patients.

IMPORTANCE AIDS-related lymphomas (ARLs) are the most common malignancies in HIV-1-infected (HIV$^+$) patients after the introduction of combined antiretroviral therapy (cART). Lymphangiogenesis is of critical importance in sustaining growth and metastasis of ARLs. Indeed, enhanced lymphangiogenesis occurs in the lymph nodes of HIV$^+$ patients under successful cART. The HIV-1 matrix protein p17 is detected in blood and accumulates in the lymph node germinal centers even in the absence of virus replication. Several findings suggest a key role for p17 as a microenvironmental factor capable of promoting lymphangiogenesis. Here, we show that p17 promotes lymphangiogenesis of human lymph node-derived lymphatic endothelial cells (LN-LECs). The lymphangiogenic activity of p17 is sustained by an autophagy-based pathway that enables LN-LECs to release prolymphangiogenic factors into the extracellular microenvironment. Our findings indicate that specific targeting of autophagy may provide an important new tool for treating ARLs.

KEYWORDS HIV-1 matrix protein p17, autophagy, lymphatic endothelial cells, lymphangiogenesis, AIDS-related lymphoma

Received 16 May 2017 **Accepted** 29 May 2017

Accepted manuscript posted online 7 June 2017

Citation Mazzuca P, Marsico S, Schulze K, Mitola S, Pils MC, Giagulli C, Guzman CA, Caruso A, Caccuri F. 2017. Role of autophagy in HIV-1 matrix protein p17-driven lymphangiogenesis. J Virol 91:e00801-17. https://doi.org/10.1128/JVI.00801-17.

Editor Guido Silvestri, Emory University

Address correspondence to Francesca Caccuri, francesca.caccuri@unibs.it.

P.M. and S.M. contributed equally to this article.

The introduction of combined antiretroviral therapy (cART) enhanced the life span of HIV-1-infected (HIV^+) patients and shifted AIDS from a fatal to a chronic syndrome (1, 2). The risk of developing tumors dramatically declined in HIV^+ patients under cART, accounting for a sustained immune reconstitution. However, the occurrence of AIDS-related lymphomas (ARLs), which comprise a narrow spectrum of histological types of high-grade and aggressively metastatic B-cell tumors, did not decrease to the same extent (3, 4). Hodgkin's lymphoma cases continue to rise, whereas non-Hodgkin's lymphoma (NHL) remains the most common malignancy in HIV^+ patients (3, 4). Furthermore, ARL cases are expected to increase in the future because HIV^+ patients are living longer on cART (5).

HIV-1 does not infect the neoplastic B cells, but lymphomagenesis seems to be hinged to the ability of HIV-1 to manipulate the host microenvironment. Lymphangiogenesis is essential in supporting proliferation and spreading of lymphomas (6), and several studies have provided evidence for an enhanced microvessel formation in lymph nodes of patients with ARLs (7). This suggests the presence of HIV-1-triggered prolymphangiogenic molecules at work in the tumor microenvironment. Several findings highlight the capability of different HIV-1 proteins to activate and sustain aberrant lymphangiogenesis (8), pointing to a need to target them for therapeutic benefit.

The HIV-1 matrix protein p17 is detected in the blood and bone marrow of HIV^+ patients (9, 10), and, together with other HIV-1 structural proteins, it accumulates in the germinal center of lymph nodes of patients under successful cART and in the absence of any *in situ* viral replication (11, 12). This is not surprising since latently HIV-1-infected resting T cells are capable of producing HIV-1 proteins without supporting spreading infection (13). Moreover, recent data show the capability of *gag*-expressing cells to release p17 in the absence of viral protease, following its cellular aspartyl protease-dependent cleavage from the *gag* precursor protein (14). Overall, these findings indicate that p17, as well as other viral structural proteins, could be produced by cells potentially residing in the germinal centers, even in the absence of viral replication.

p17 has a well-established role in the virus life cycle (15). Extracellularly, the viral protein displays potent angiogenic and lymphangiogenic activity, and its ability to promote the formation of mature neovessels (vasculogenesis) was found as potent as that exerted by vascular endothelial growth factor A (VEGF-A) (16, 17). The activity of p17 occurs after binding to the chemokine (C-X-C motif) receptor 1 (CXCR1) and CXCR2 expressed on endothelial cells (ECs), thus mimicking the prolymphangiogenic activity of the CXCR1/2 natural ligand interleukin-8 (18). However, we also observed that p17-induced lymphangiogenesis was mediated, at least in part, by the release of endothelin 1 (ET-1) and by activation of the ET-1/ET-1 B receptor axis (17). This finding prompted us to investigate the role of secretory pathways in sustaining the lymphangiogenic activity of the viral protein.

In this study, we demonstrate that the lymphangiogenic activity of p17 occurs on human lymph node-derived lymphatic endothelial cells (LN-LECs) only under stress conditions, such as serum nutrient starvation, and relies entirely on mechanisms of autophagy. Moreover, p17 vasculogenic activity *in vivo* is totally impaired in autophagy-incompetent mice. These findings open new opportunities to gain deep insight into mechanisms underlying the lymphangiogenic and vasculogenic activity of p17 and to identify novel treatment strategies in fighting ARLs.

RESULTS

The lymphangiogenic activity of p17 occurs under stress conditions. p17 strongly induces lymphangiogenesis in serum-starved LN-LECs (17). In order to understand if serum starvation is a *conditio sine qua non* for p17 activity, we performed a dose-response tube formation experiment on LN-LECs under normal (Fig. 1A) or serum-deprived (Fig. 1B) conditions. LN-LECs were seeded on 48-well plates (5×10^4 cells per well) containing polymerized plugs of growth factor-reduced Cultrex basement membrane extract (BME) in the presence or absence of different doses of p17. Under normal culture conditions, p17 did not promote lymphangiogenesis at any dose

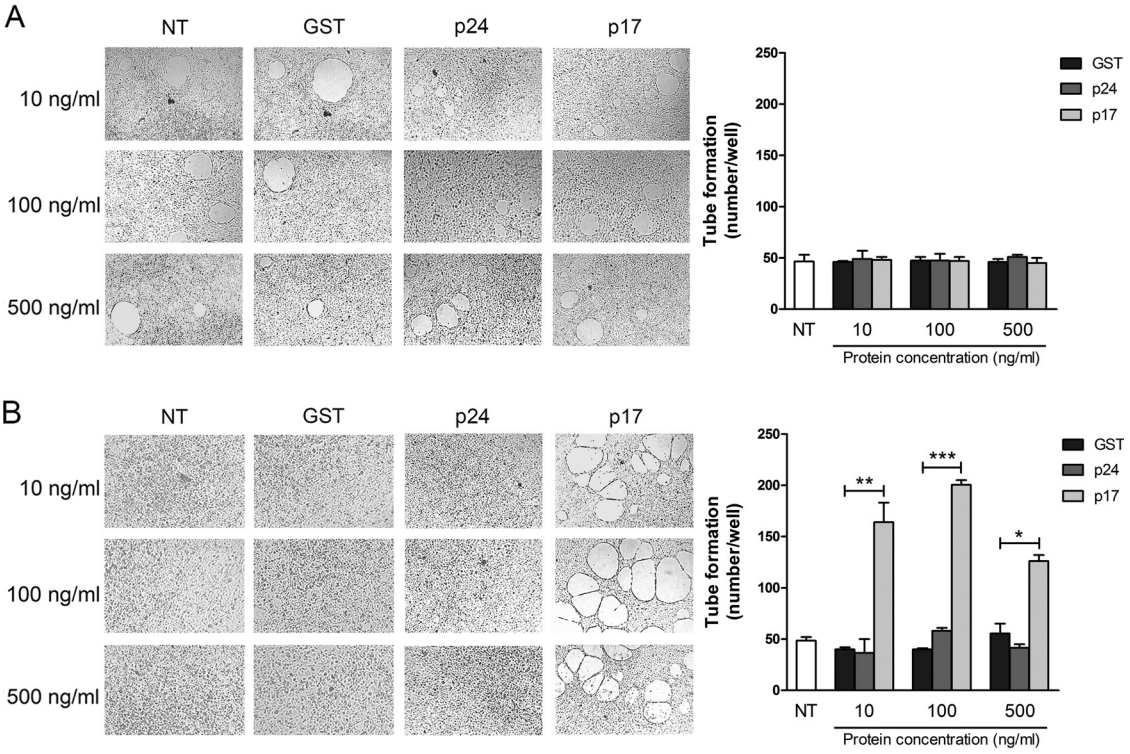

FIG 1 Tube formation induced by p17 requires stressed LN-LEC conditions. Tube formation of LN-LECs is shown in response to the indicated treatments. Pictures were taken after 12 h of culture on growth factor-reduced Cultrex BME (magnification, ×10). (A) LN-LECs were cultured in complete medium and then stimulated for 12 h with 10, 100, and 500 ng/ml of GST, p24, or p17. (B) LN-LECs were serum starved for 16 h with EBM containing 0.5% FBS and then stimulated as described above in complete medium. Values reported for tube formation are the means ± SDs of three independent experiments with similar results. Statistical analysis was performed by one-way ANOVA; a Bonferroni posttest was used to compare data (*, $P < 0.05$; **, $P < 0.01$; ***, $P < 0.001$). NT, not treated.

tested compared to results in cells not treated (NT) or treated with the irrelevant protein glutathione *S*-transferase (GST) or p24 (Fig. 1A). On the contrary, LN-LECs cultured for 16 h under serum-deprived conditions were highly susceptible to stimulation with p17, demonstrating that it exerts a potent lymphangiogenic activity on LN-LECs cultured under stress, i.e., nutrient starvation, conditions only. This activity was evident at all tested doses, with the maximum effect reached at 100 ng/ml (Fig. 1B). Since we previously showed that exogenous p17 is present in the serum of HIV$^+$ patients at nanomolar concentrations (10) and having consistently employed 10 ng/ml of p17 for proving its involvement in lymphangiogenesis (17), we have chosen this protein concentration to perform all subsequent experiments.

Inhibition of autophagy decreased p17-triggered lymphangiogenesis. Autophagy is a dynamic process of subcellular degradation that is critical for maintaining cell metabolism and survival (19). Recently, a positive link between autophagy and angiogenesis under different stress conditions has become evident (20, 21). Thus, we wondered whether the lymphangiogenic activity of p17 on LN-LECs cultured under serum deprivation could be attributed to autophagy. We used 3-methyladenine (3-MA), a synthetic and cell-permeable autophagic sequestration blocker (22), to pharmacologically inhibit autophagy. LN-LECs were starved for 16 h in the presence or absence of 3-MA (5 mM), and then a tube-like structure formation assay was performed in unstimulated cells or in cells stimulated for 12 h with 10 ng/ml of p17. As shown in Fig. 2A, inhibition of autophagy with 3-MA strongly decreased the p17 lymphangiogenic activity. The activity of p17 was blocked by preincubating the medium containing p17 with the neutralizing monoclonal antibody (MAb) MBS-3 (1 μg/ml) whereas incubation with an irrelevant control MAb (1 μg/ml) had no effect, thus confirming the specificity of the p17 biological activity (Fig. 2A).

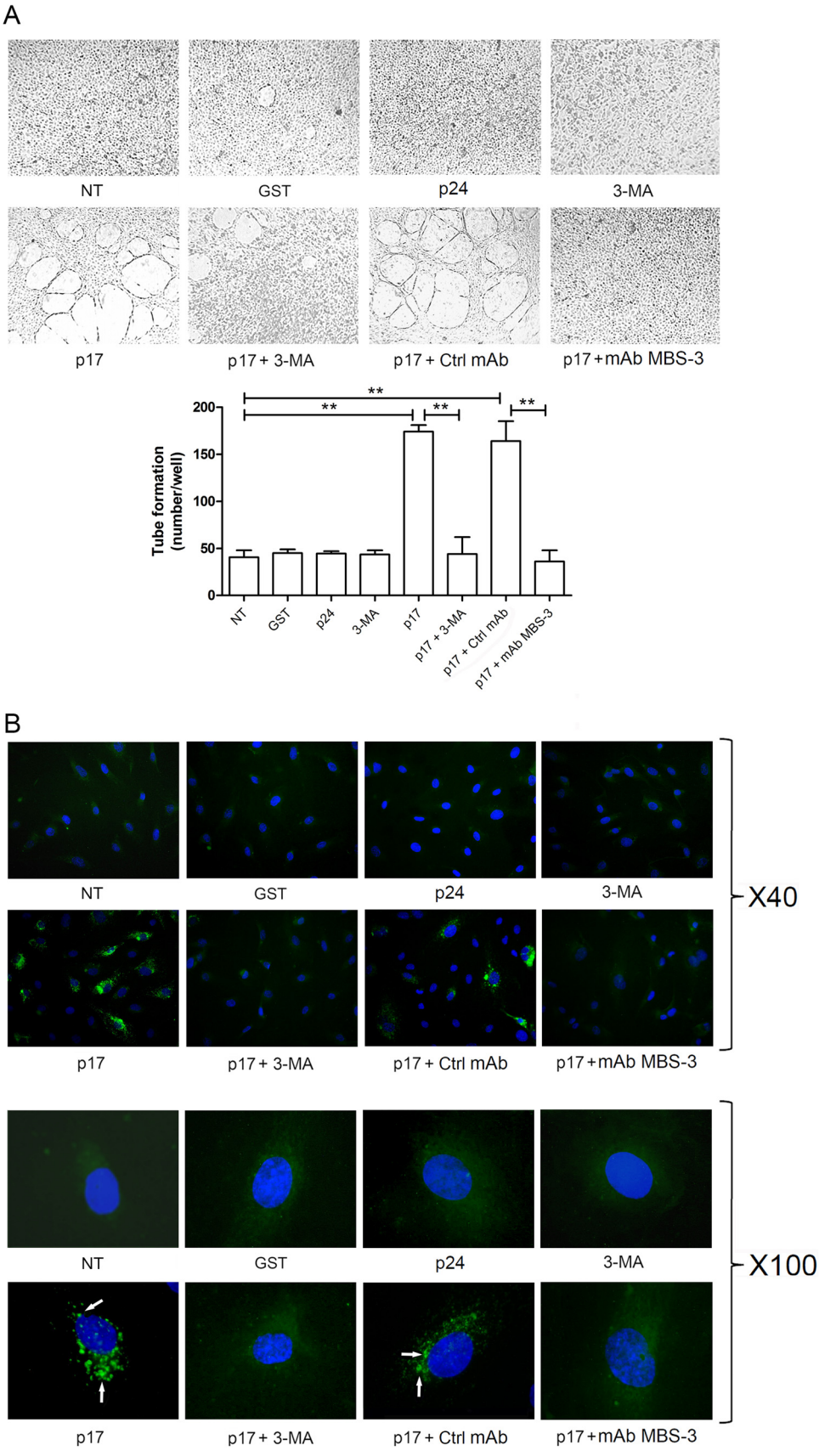

FIG 2 Inhibition of autophagy with 3-MA decreases p17-mediated lymphangiogenesis. (A) LN-LECs were starved for 16 h and then left unstimulated or stimulated or with 10 ng/ml of GST, p24, or p17 in complete medium.

(Continued on next page)

Microtubule-associated protein 1A/1B-light chain 3 (LC3) is a cellular protein involved in autophagosome formation. During autophagy, a cytosolic form of LC3 linked to phosphatidylethanolamine is recruited to autophagosomal membranes. Thus, detection of LC3 by immunofluorescence has become a reliable method for monitoring autophagy-related processes (23). Here, we used an enhanced green fluorescent protein (EGFP)-LC3-expressing plasmid to transfect LN-LECs and monitor autophagosome formation by the appearance of bright green punctate fluorescence in the cytoplasm (24, 25). Twenty-four hours after nucleofection, LN-LECs were serum starved for 16 h with or without 3-MA (5 mM) and then cultured for 3 h in endothelial growth medium (EGM) containing 10% fetal bovine serum (FBS) in the presence or absence of stimuli. Even though serum starvation for 16 h was expected to induce autophagy, serum-starved LN-LECs (NT) did not show activation of autophagy, at least at appreciable levels. Indeed, NT cells showed a diffuse cytoplasmic fluorescence in the presence of rare, if any, LC3-positive ($LC3^+$) autophagosome formation (Fig. 2B). At the same time, stimulation of serum-starved LN-LECs with p17 strongly promoted $LC3^+$ autophagosome formation, whereas cells stimulated with the irrelevant proteins GST and p24 did not. Upon p17 stimulation, punctate LC3-expressing structures were few and appeared as spots located near the plasma membrane. As expected, pharmacologic inhibition of autophagy with 3-MA completely blocked the p17-triggered dot-like LC3 expression. Specificity of p17 activity was demonstrated by blocking LC3 dot-like structures by preincubating p17 with the neutralizing MAb MBS-3 (Fig. 2B). These data suggest that autophagy sustains the lymphangiogenic activity of p17.

p17 promotes autophagy by interacting with CXCR1 and CXCR2. The lymphangiogenic response of LN-LECs to p17 requires activation of both CXCR1 and CXCR2 (17). Therefore, we determined the involvement of both receptors in p17-induced autophagy by examining the effect exerted by neutralizing MAbs to CXCR1 and CXCR2. As shown in Fig. 3A, serum-starved LN-LECs formed capillary-like structures after 12 h of culture in medium containing p17 or p17 plus the isotype-matched MAb (Ctrl MAb; 2.5 μg/ml). The neutralizing MAb to CXCR1 (2.5 μg/ml) was strongly inhibitory (70.1% $\pm$ 4.3%) toward p17-induced capillary-like structure formation, whereas the neutralizing MAb to CXCR2 (2.5 μg/ml) accounted for a smaller decrease (20.5% $\pm$ 4.7%). Blocking both receptors by using a combination of the two MAbs (1.25 μg/ml of each MAb) resulted in almost complete inhibition (86.4% $\pm$ 2.5%). According to our previous results (17), data presented here show that both CXCR1 and CXCR2 are involved in p17-induced capillary-like structure formation, with a major role for CXCR1 in mediating the p17 lymphangiogenic activity. At the same time, when neutralizing MAbs to CXCR1 and CXCR2 were combined, they completely blocked the p17-triggered dot-like LC3 expression, whereas an irrelevant control MAb (Ctrl MAb) had no effect (Fig. 3B). Altogether, these findings demonstrate that both chemokine receptors cooperate in sustaining the lymphangiogenic activity of p17 through activation of autophagy in human LN-LECs.

FIG 2 Legend (Continued)

LN-LECs were starved for 16 h in the presence or absence of 3-MA (5 mM), as indicated. In selected experiments, LN-LECs were stimulated with p17 (10 ng/ml) after preincubation of the viral protein with 1 μg/ml of MAb to p17 (MAb MBS-3) or an unrelated control MAb (Ctrl MAb) for 30 min at 37°C. Pictures were taken after 12 h of culture on growth factor-reduced Cultrex BME (magnification, $\times$10) and are representative of three independent experiments with similar results. Values reported for tube formation are the means $\pm$ SDs of three independent experiments with similar results. Statistical analysis was performed by one-way ANOVA; a Bonferroni posttest was used to compare data (**, $P < 0.01$). (B) LN-LECs were nucleofected with EGFP-LC3 plasmid, and 24 h after nucleofection cells were starved for 16 h and then left unstimulated or stimulated with 10 ng/ml of GST, p24, or p17 for 3 h in complete medium. When indicated, LN-LECs were starved for 16 h in the presence or absence of 3-MA (5 mM). In selected experiments, LN-LECs were stimulated with p17 (10 ng/ml) after preincubation of the viral protein with 1 μg/ml of MAb to p17 (MAb MBS-3) or an unrelated control MAb (Ctrl MAb) for 30 min at 37°C. The images display LC3 signals in green and cell nuclei in blue. Magnification is as indicated on the figure. Green-positive punctate structures were counted in order to quantify relative levels of autophagy. The percentage of positive cells was calculated for 10 independent fields at a magnification of $\times$40. A total number of 29 $\pm$ 10 cells per microscope field was counted, and the percentage of LC3-positive punctate cells under p17 stimulation was found to be 38% $\pm$ 3%. White arrows indicate dot-like $LC3^+$ structure formation. NT, not treated.

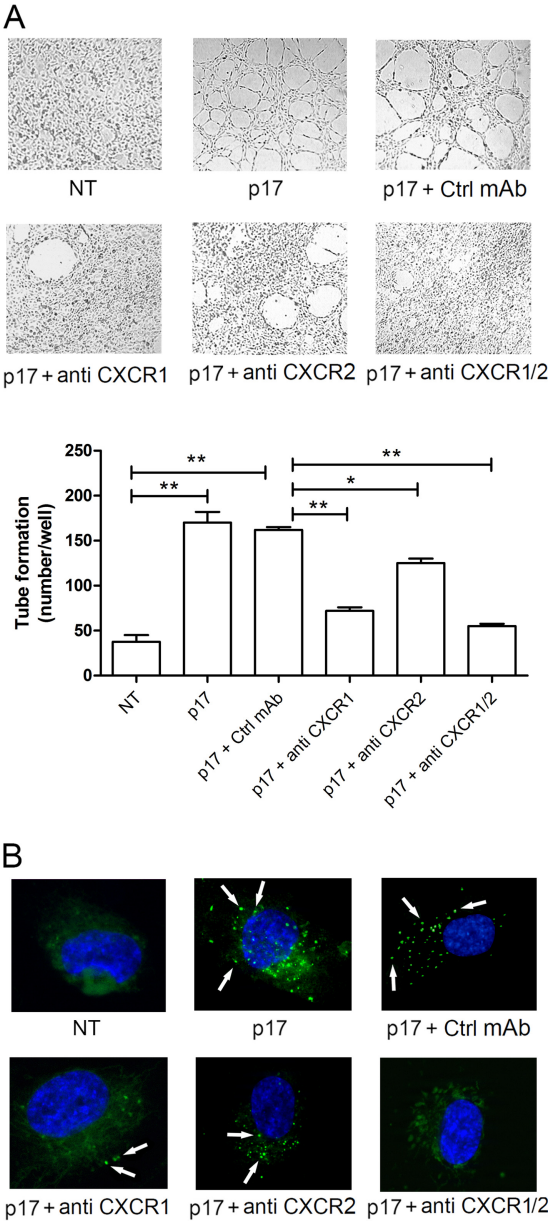

FIG 3 CXCR1 and CXCR2 drive the autophagy-based activity of p17. (A) LN-LECs were starved for 16 h and then stimulated or not with p17 (10 ng/ml) in complete medium. Starved cells were pretreated for 1 h at 37°C with 2.5 μg/ml of an isotype-matched MAb (Ctrl MAb), a neutralizing MAb to CXCR1 (anti-CXCR1), and/or a neutralizing MAb to CXCR2 (anti-CXCR2), as indicated, before p17 stimulation. Pictures were taken after 12 h of culture on growth factor-reduced Cultrex BME (magnification, $\times$10) and are representative of three independent experiments with similar results. Values reported for tube formation are the means $\pm$ SDs of three independent experiments with similar results. Statistical analysis was performed by one-way ANOVA; a Bonferroni posttest was used to compare data (*, $P < 0.05$; **, $P < 0.01$). (B) LN-LECs were nucleofected with EGFP-LC3 plasmid and, 24 h after nucleofection, incubated in serum-deprived medium for 16 h. Cells were then stimulated with p17 (10 ng/ml) for 3 h in complete medium. Starved cells were pretreated for 1 h at 37°C with 2.5 μg/ml of an isotype-matched MAb (Ctrl MAb), a neutralizing MAb to CXCR1 (anti-CXCR1), and/or a neutralizing MAb to CXCR2 (anti-CXCR2), as indicated, before p17 stimulation. The images display LC3 signals in green and cell nuclei in blue. Magnification, $\times$100. White arrows indicate dot-like LC3$^+$ structure formation. NT, not treated.

Autophagy promoted by p17 is Beclin-1 dependent. To confirm the involvement of autophagy in p17 lymphangiogenic activity, we inhibited by small interfering RNA (siRNA) the expression of Beclin-1 (siBeclin), a coiled-coil protein involved in the regulation of autophagy in mammalian cells (26–28). LN-LECs were nucleofected with

siBeclin and with a scrambled irrelevant siRNA (siScramble) as a negative control. We obtained 60% of silencing efficacy, as confirmed by Western blotting (Fig. 4A). Twenty-four hours after nucleofection, cells were serum starved for 16 h and then left unstimulated or stimulated with p17 or with the irrelevant proteins GST and p24. As shown in Fig. 4B, mock-silenced LN-LECs (siScramble) were able to form capillary-like structures upon p17, but not GST and p24, stimulation. At the same time, silencing of Beclin-1 drastically inhibited tube-like structure formation triggered by p17, with similar numbers of tubes/well observed in Beclin-1-silenced LN-LECs (siBeclin) stimulated or not with the irrelevant proteins, as shown by the almost superimposable images. As expected, no effect on LC3 expression as punctate dots was observed in siBeclin LN-LECs treated or not with GST or p24. At the same time, inhibition of autophagy by silencing Beclin-1 impaired the formation of punctate structures in siBeclin LN-LECs stimulated with p17 (Fig. 4C). Therefore, both pharmacologic and genetic tools are aligned in confirming the capability of p17 to promote lymphangiogenesis through induction of autophagy.

Autophagy regulates LN-LEC migration triggered by p17. Since migration of ECs under stress conditions is promoted by autophagy (29), we scrutinized the involvement of autophagy in the LN-LEC migratory activity promoted by p17 using a wound-healing assay. LN-LECs were grown on collagen-coated plates and serum starved for 16 h in the presence or absence of 3-MA (5 mM). Confluent cell monolayers were scratched with a 200-μl pipette tip, and the percentage of wound healing was observed over a period of 12 h. As shown in Fig. 5, untreated LN-LECs (NT) reached a level of approximately 45% (standard deviation [SD], $\pm$6%) healing after 12 h of culture, similar to cells treated with the irrelevant proteins GST or p24 (42% $\pm$ 3% and 47% $\pm$ 4%, respectively). At the same time, LN-LECs treated with p17 reached 100% healing, showing a considerable improvement in their wound repair ability. In contrast, LN-LECs pretreated with 3-MA and stimulated with p17 reached approximately 42% ($\pm$5%) healing, almost equivalent to that of LN-LECs pretreated with 3-MA alone (41% $\pm$ 5% SD). These results demonstrate that inhibition of autophagy decreases migratory activity of LN-LECs triggered by p17.

ET-1 secretion triggered by p17 is autophagy dependent. Our previous study demonstrated that p17 stimulates ET-1 secretion, which is responsible, at least in part, for p17-mediated lymphangiogenesis through a paracrine activation of the ET-1 B receptor (17). To investigate the role of autophagy in this p17 activity, we performed a kinetic study by collecting supernatants of serum-starved LN-LECs for 16 h in the presence or absence of 3-MA (5 mM) and then culturing LN-LECs for 1, 3, and 6 h in complete medium either not supplemented or containing 10 ng/ml of GST, p24, or p17. As shown in Fig. 6, p17 induced a significant increase of ET-1 secretion at 3 and 6 h of LN-LEC stimulation compared to levels in cells not treated (NT) or treated with the irrelevant proteins GST and p24. At the same time, p17-triggered ET-1 secretion was significantly inhibited by pretreatment of LN-LECs with 3-MA, whereas 3-MA alone did not induce any increase in ET-1 release (Fig. 6). These data show that ET-1 secretion by LN-LECs stimulated with p17 is dependent on activation of an autophagy-based pathway.

The lymphangiogenic activity of p17 depends on GRASP55, Rab8a, and cathepsin-β status. Further experiments were then run to support the key role played by autophagy in p17-mediated lymphangiogenesis. We first performed silencing of two important genes involved in autophagy, namely, GRASP55 (30–32) and Rab8a (32). GRASP55 is a "Golgi reassembly stacking protein" involved in lateral organization of Golgi ribbons. It is the only specific marker thus far known to be essential for autophagy-based protein secretion. The crucial role of GRASP55 in autophagosome formation but not in maturation has recently been demonstrated, thus establishing its regulating role in the first phase of autophagy (32). Rab8a is a small GTPase that is a component of the vectorial vesicular transport system to the plasma membrane; it participates in autophagy-based secretion and plays a crucial role in the activation of Beclin-1-dependent autophago-

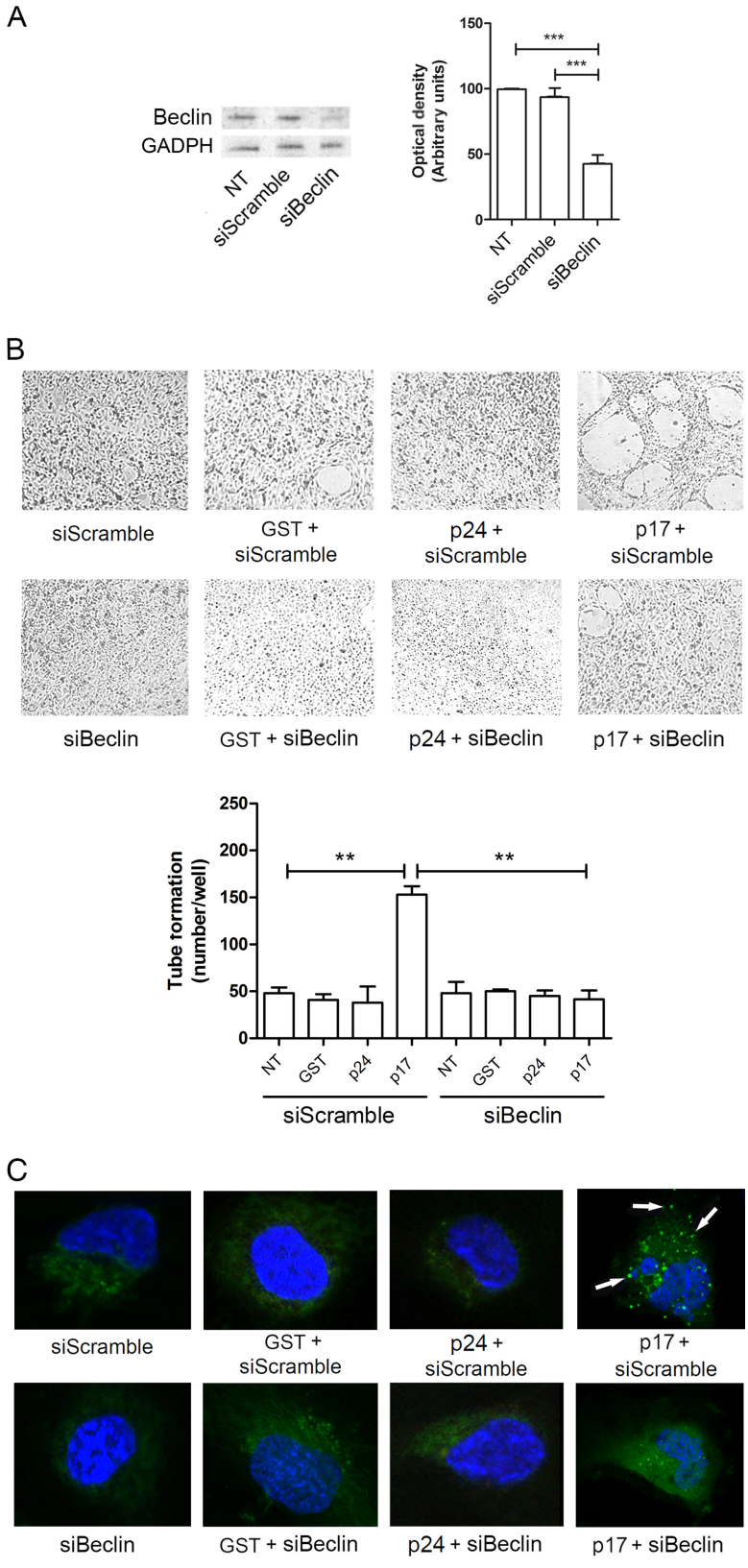

FIG 4 Role of Beclin-1 in p17-induced lymphangiogenesis. (A) Immunoblotting analysis of Beclin-1 knockdown cells. Blots from one representative experiment out of three with similar results are shown (left). Values reported for Beclin-1 are the means ± SDs of three independent experiments (right). Statistical analysis was performed by one-way ANOVA; a Bonferroni posttest was used to compare data (***, $P < 0.001$). (B) LN-LECs were nucleofected with Beclin-1 and irrelevant (siScramble) siRNAs.

(Continued on next page)

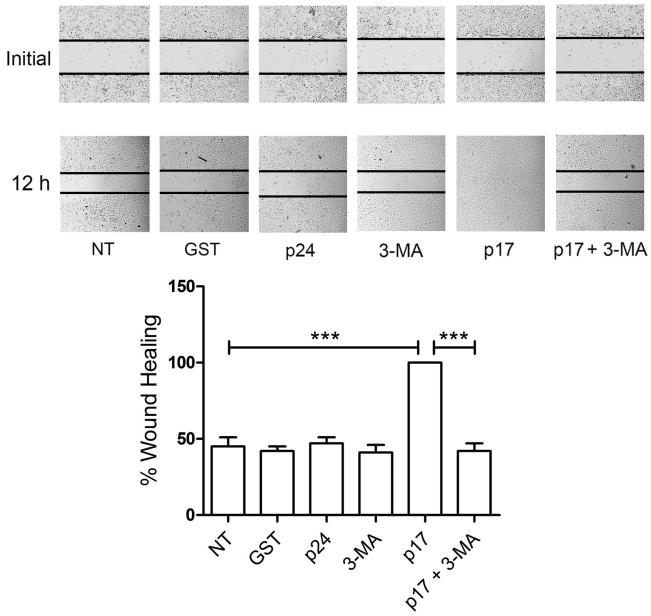

FIG 5 Autophagy sustains p17-triggered LN-LEC migration. LN-LECs were serum starved for 16 h in the presence or absence of 3-MA (5 mM). Confluent LN-LEC monolayers were scratched using a 200-μl pipette tip and cultured for 6 h in complete medium either unsupplemented or containing 10 ng/ml of GST, p24, or p17. Images are representative of three independent experiments with similar results (magnification, $\times$10). Statistical analysis was performed by one-way ANOVA; a Bonferroni posttest was used to compare data (***, $P < 0.001$). NT, not treated.

some assembly (33). The efficacy of silencing was approximately 50% for both genes as assessed by Western blotting (Fig. 7A and B, upper panels). As shown in Fig. 7A and B (lower panels), silencing of each gene in serum-starved LN-LECs was sufficient to reduce tube formation promoted by p17 stimulation. As expected, no effect on tube formation was observed in siGRASP55 and siRab8a LN-LECs either untreated or treated with GST or p24. Then, we pharmacologically inhibited cathepsin-β through the specific inhibitor CA-074Me. Since the autophagy-driven secretion of proteins and cytokines is accomplished by cathepsin-β (32), a lysosomal enzyme, we tested the lymphangiogenic activity of p17 in the presence of different doses of CA-074Me. As shown in Fig. 7C, CA-074Me was able to inhibit the lymphangiogenic activity of p17 at all doses tested. Moreover, inhibition of GRASP55, Rab8a, and cathepsin-β activity resulted in inhibition of p17-induced ET-1 secretion (Fig. 7D). Altogether, our data further confirm the key role played by autophagy in supporting the lymphangiogenic activity of p17.

The vasculogenic activity of p17 is abolished in BECN-1 KO mice. We previously reported that p17 and ET-1 are capable of stimulating neovessel formation *in vivo* (16, 17, 34). To confirm the involvement of autophagy in sustaining p17 vasculogenic activity, we implanted Matrigel containing p17, ET-1, or phosphate-buffered saline (PBS; negative control) into the dorsal subcutaneous tissue of wild-type (WT) C57BL/6 (autophagy competent) or Beclin-1 knockout (BECN-1 KO; autophagy incompetent)

FIG 4 Legend (Continued)
Twenty-four hours after nucleofection, cells were serum starved for 16 h and then seeded on growth factor-reduced Cultrex BME in the presence or absence of 10 ng/ml of GST, p24, or p17. Pictures were taken after 12 h of culture on growth factor-reduced Cultrex BME (magnification, $\times$10). Values reported for tube formation are the means $\pm$ SDs of three independent experiments with similar results. Statistical analysis was performed by one-way ANOVA; a Bonferroni posttest was used to compare data (**, $P < 0.01$). (C) LN-LECs were conucleofected with EGFP-LC3 plasmid and siScramble or with EGFP-LC3 plasmid and siBeclin-1. Twenty-four hours after nucleofection, cells were incubated for 16 h in serum-starved medium and then left untreated or treated for 3 h with 10 ng/ml of GST, p24, or p17 in complete medium. The images display LC3 signals in green and cell nuclei in blue. Magnification, $\times$100. White arrows indicate dot-like LC3$^+$ structure formation. NT, not treated.

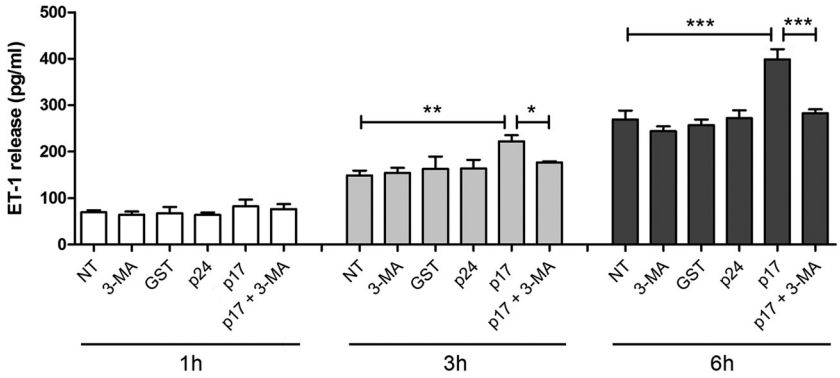

FIG 6 Role of autophagy in p17-mediated release of ET-1. LN-LECs were serum starved for 16 h in the presence or absence of 3-MA (5 mM). After starvation, LN-LECs were cultured in complete medium either unsupplemented or containing 10 ng/ml of GST, p24, or p17. Supernatants were collected at 1, 3, and 6 h of culture and analyzed for the presence of ET-1 by a standard quantitative ELISA. Bars represent the means ± SDs of triplicate samples. Statistical analysis was performed by one-way ANOVA separately for each concentration of p17 across the three groups. A Bonferroni posttest was used to compare data (*, $P < 0.05$; **, $P < 0.01$; ***, $P < 0.001$). NT, not treated.

mice. As expected, immunostaining of Matrigel plugs with a rat MAb to mouse CD31, a pan-endothelial marker, identified pronounced numbers of CD31-positive capillary structures in p17- and ET-1-containing Matrigel plugs implanted in C57BL/6 WT mice (Fig. 8B and C, respectively). Staining was confined within discrete areas at the boundaries with the surrounding murine tissue. On the other hand, no capillary-like structure was detected in the p17-containing Matrigel plugs implanted in autophagy-incompetent BECN-1 KO mice (Fig. 8E), nor in implants of either WT or BECN-1 KO mice containing PBS (Fig. 8A and D). Different results were obtained with ET-1, whose implants in BECN-1 KO mice showed a consistent number of CD31-positive capillary structures (Fig. 8F). This finding attests to the prominent role of autophagy in sustaining the vasculogenic activity of p17. Interestingly, our data demonstrate, for the first time, that the ET-1 vasculogenic activity is independent of autophagy *in vivo*.

Autophagy supports the lymphangiogenic activity of a B-cell growth-promoting p17 variant. Distinct p17 variants with enhanced B-cell-activating and growth-promoting properties have been detected in patients with NHL (35, 36). These variants usually carry insertions at the C-terminal region, which were shown to specifically induce structural destabilization of the viral protein (35). In order to understand if these p17 variants with B-cell clonogenic activity were also capable of supporting lymphangiogenesis by activation of secretory autophagy, we tested the lymphangiogenic activity of a p17 variant named NHL-a105, derived from an HIV$^+$ patient with NHL (35). As shown in Fig. 9, the p17 variant NHL-a105 was extremely potent in promoting tube formation. This occurred, as for p17, under serum-starved conditions only (Fig. 9A). Similarly to p17, NHL-a105 was performing its activity on LN-LECs by activation of autophagy. In fact, the lymphangiogenic activity triggered by NHL-a105 was drastically impaired in serum-starved LN-LECs pretreated with 3-MA (5 mM) or silenced for Beclin-1 (Fig. 9B). Both genetic (GRASP55 and Rab8a silencing) and pharmacologic (cathepsin-β) inhibition of autophagy strongly reduced the NHL-a105 lymphangiogenic activity (Fig. 9C), further confirming the involvement of autophagy in sustaining the lymphangiogenic activity of this p17 variant. Moreover, NHL-a105-induced ET-1 secretion by serum-starved LN-LECs was abolished by pharmacologic or genetic inhibition of autophagy (Fig. 9D). These findings confirm the capability of the B-cell clonogenic p17 variant NHL-a105 to support lymphangiogenesis by activating an autophagy-based pathway.

DISCUSSION

ARL cases are expected to increase in the future because HIV$^+$ patients are living longer on cART (5) and because cART was not found to have an impact on lymphoma

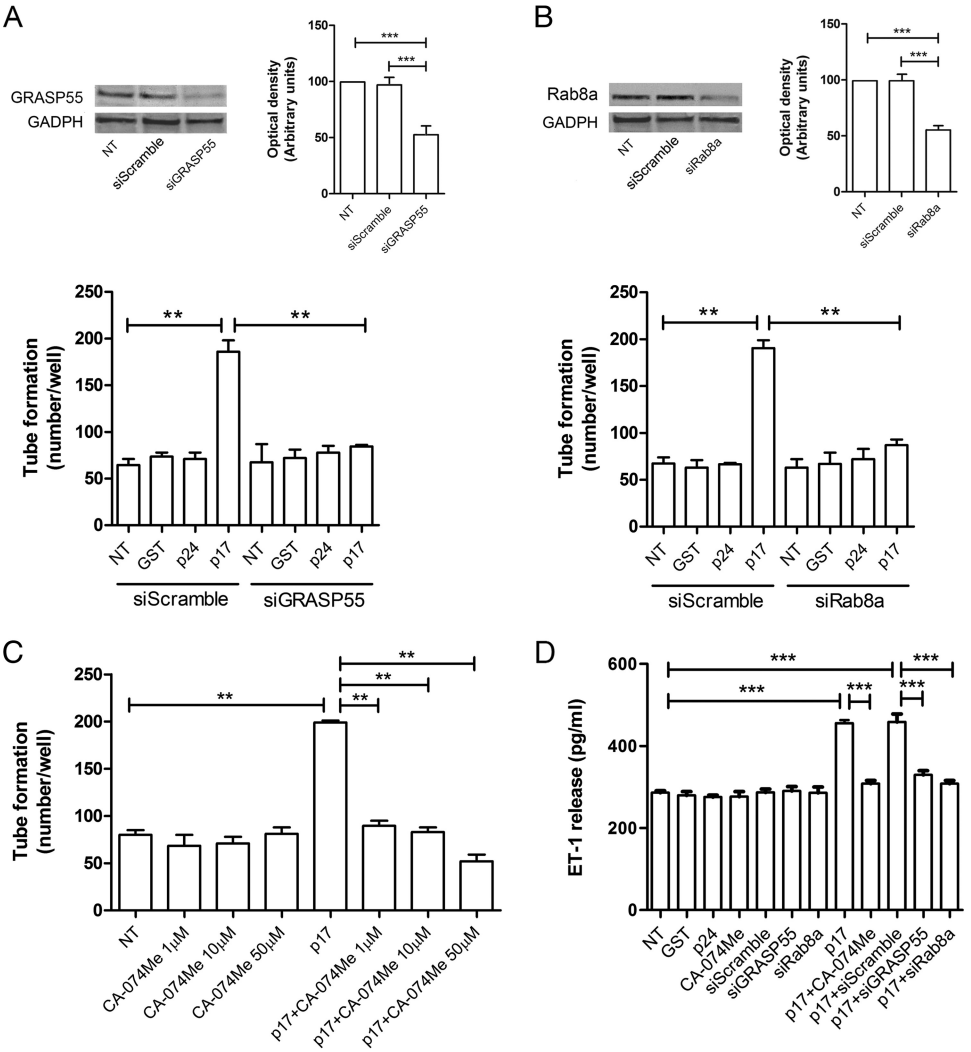

FIG 7 Mechanistic insight into the prolymphangiogenic activity of p17. LN-LECs were nucleofected with siGRASP55, siRab8a, and siScramble. (A and B) Immunoblotting analysis was performed on LN-LECs at 24 h after GRASP55 (A, upper panel) or Rab8a (B, upper panel) siRNA nucleofection. Blots from one representative experiment of three with similar results are shown. Values reported for GRASP55 or Rab8a knockdown are the means ± SDs of three independent experiments with similar results. Twenty-four hours after nucleofection, cells were serum starved for 16 h, and then a tube formation assay was performed with either untreated LN-LECs or with siScramble-nucleofected LN-LECs or LN-LECs silenced for GRASP55 (A, lower panel) or Rab8a (B, lower panel) with 10 ng/ml of GST, p24, or p17 in complete medium. (C) Tube formation assay of LN-LECs serum starved for 16 h in the presence or absence of 1, 10, and 50 μM CA-074Me (cathepsin-β inhibitor) and then seeded on growth factor-reduced Cultrex BME-coated wells and either untreated or treated with p17 (10 ng/ml) in complete medium. Values reported for tube formation are the means ± SDs of three independent experiments with similar results. (D) LN-LECs were serum starved in the presence or absence of 50 μM CA-074Me. In some experiments, LN-LECs were nucleofected with siScramble, siGRASP55, or siRab8a, and 24 h after nucleofection, cells were serum starved for 16 h. After starvation, LN-LECs were cultured in complete medium either unsupplemented or containing 10 ng/ml of GST, p24, or p17. After 6 h of culture, supernatants were collected and analyzed by a standard quantitative ELISA. Bars represent the means ± SDs of triplicate samples. Statistical analysis was performed by one-way ANOVA; a Bonferroni posttest was used to compare data (**, $P < 0.01$; ***, $P < 0.001$). NT, not treated.

development, in contrast to what was observed for other tumors (3, 4). Furthermore, ARLs are usually high grade and aggressively metastatic (37), usually arising systemically and having a poor prognosis (38, 39). Enhanced microvessel formation in lymph nodes of patients with ARLs has been clearly documented (7), and the hypothesis that p17 may be a key player in supporting lymphomagenesis is becoming one of the most consistent. In fact, the viral matrix protein is detected in the microenvironment even in the absence of virus replication (9, 13). p17 accumulates and persists in the germinal center of lymph nodes even in patients under successful cART (10, 11) and exerts lymphangiogenic activity both *in vitro* and *in vivo* (17, 34).

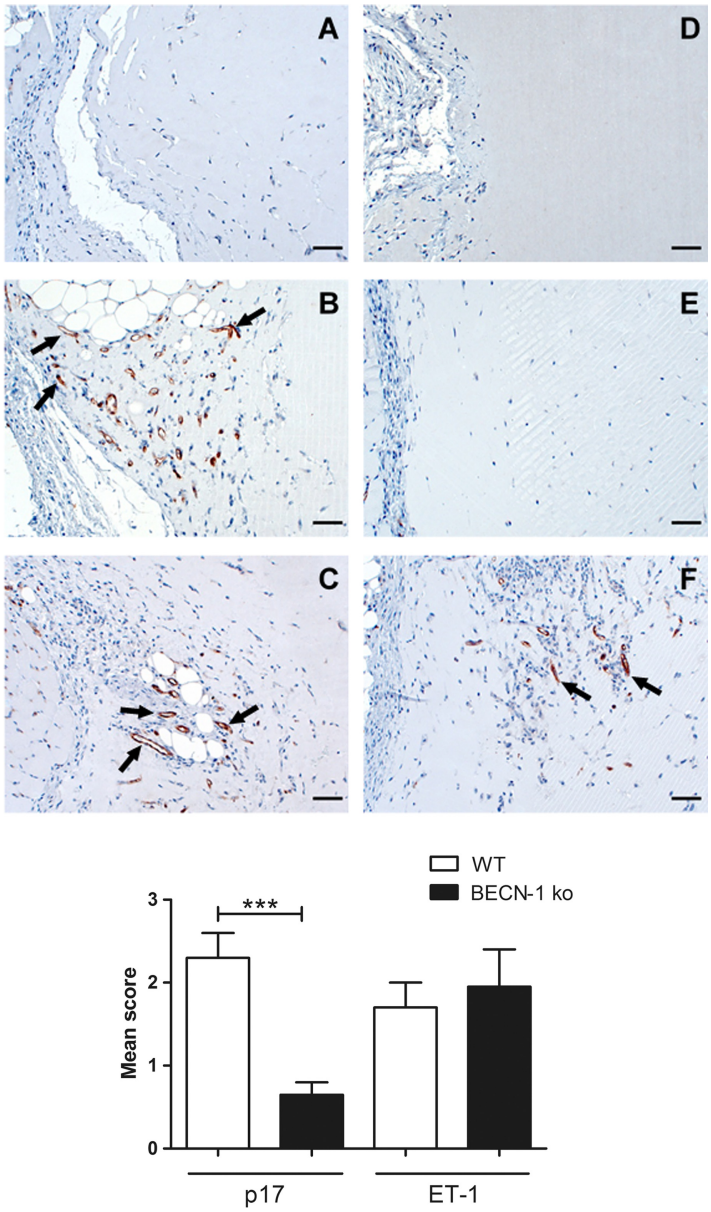

FIG 8 p17-mediated *in vivo* vasculogenesis is abolished in BECN-1 KO mice. Ten days after subcutaneous injection of growth factor-reduced Cultrex BME plugs containing PBS, p17 (200 ng/ml), or ET-1 (200 ng/ml), the implants were immunostained with a MAb to mouse CD31. Neovessel formation (arrows) occurs in implants of wild-type (WT) mice containing p17 (B) or ET-1 (C) and in implants of BECN-1 KO mice containing ET-1 (F). Neovessels were absent in implants of BECN-1 KO mice containing p17 (E) as well as in implants of both WT and BECN-1 KO mice containing PBS (A and D). Representative figures for each group are shown. Scale bar, 50 μm. A semiquantitative score was applied for the amount of CD31-positive cells in the implant: 0, no positive cells; 1, a single positive cell with moderate staining intensity; 2, one focus of more than 5 to 30 positive cells; 3, two or more foci of more than 30 positive cells. The standard error of mean is indicated by vertical lines. Statistical analysis was performed by one-way ANOVA; a Bonferroni posttest was used to compare data (***, $P < 0.001$).

Autophagy has been very recently described to occur in human LN-LECs, attesting to a role for autophagy in tuberculosis pathogenesis (40). In particular, upon infection, autophagy is induced, and autophagosomes are formed in LN-LECs, leading to an autophagic degradation flux that in some instances can be overcome by the pathogen (40). Here, we show for the first time that autophagy and possibly secretory autophagy sustain p17-triggered lymphangiogenesis. Indeed, induction of autophagy by p17 promotes potent lymphangiogenesis, whereas pharmacological and genetic inhibition

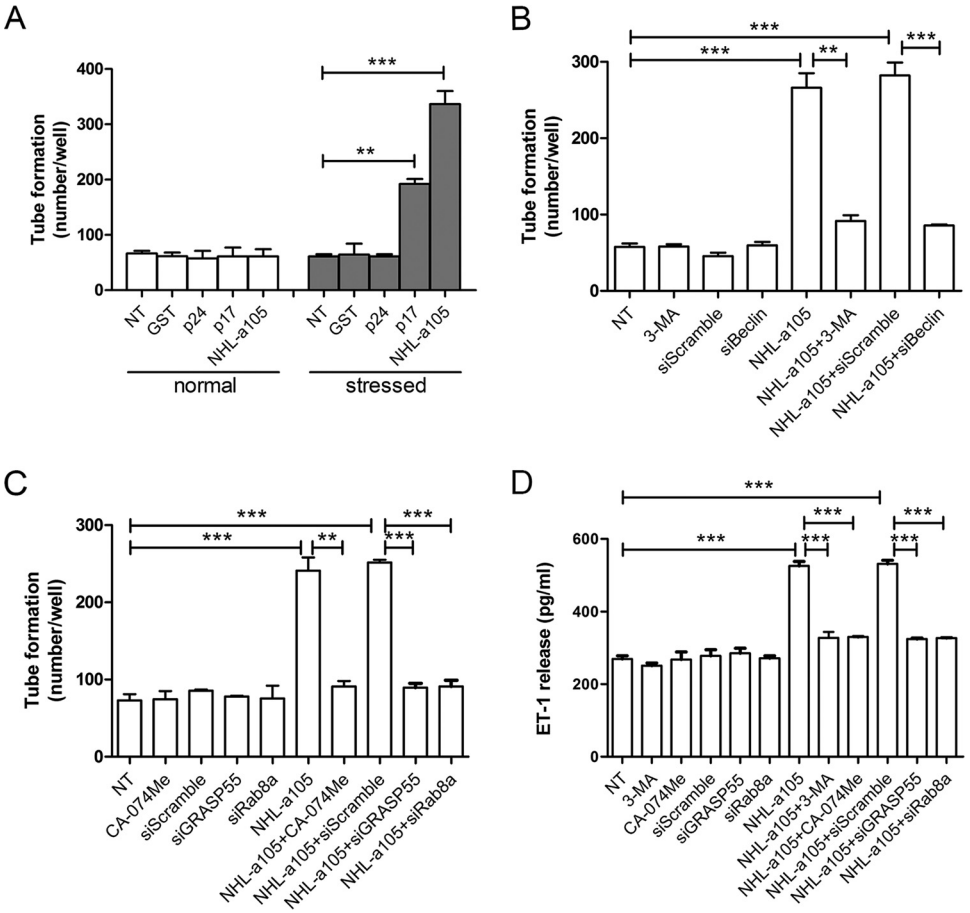

FIG 9 The lymphangiogenic activity of a B-cell growth-promoting p17 variant (NHL-a105) is supported by autophagy. (A) LN-LECs were cultured for 16 h in complete medium (normal) or under serum-starved (stressed) conditions and then cultured for 12 h in the absence or presence of 10 ng/ml of GST, p24, p17, or NHL-a105 in complete medium. (B) LN-LECs were serum starved for 16 h in the presence or absence of 3-MA (5 mM) or after nucleofection with siScramble or siBeclin-1. After starvation, LN-LECs were stimulated or not with NHL-a105 (10 ng/ml). (C) Tube formation assay of LN-LECs serum starved for 16 h in the presence or absence of CA-074Me (50 μM) or serum-starved LN-LECs after nucleofection with siScramble, siGRASP55, or siRab8a. Cells were then treated or not for 12 h with NHL-a105 (10 ng/ml). Values reported for tube formation are the means $\pm$ SDs of three independent experiments with similar results. Statistical analysis was performed by one-way ANOVA; a Bonferroni posttest was used to compare data. (D) LN-LECs were serum starved for 16 h in the presence or absence of 3-MA (5 mM) or CA-074Me (50 μM). In some experiments, LN-LECs were nucleofected with siScramble, siGRASP55, or siRab8a for 24 h and then serum starved for 16 h. Then, cells were treated or not with 10 ng/ml of NHL-a105. After 6 h of stimulation, culture supernatants were collected and analyzed for the presence of ET-1 by quantitative ELISA. Bars represent the means $\pm$ SDs of triplicate samples. Statistical analysis was performed by one-way ANOVA. A Bonferroni posttest was used to compare data (**, $P < 0.01$; ***, $P < 0.001$). NT, not treated.

of autophagy suppress it. Moreover, our data agree with previous studies performed on vascular ECs showing that inhibition of autophagy by 3-MA reduces tube formation and cell migration, whereas induction of autophagy enhances these angiogenic functions (19). Data obtained on autophagy-incompetent Beclin-1 knockout mice further highlight the role of autophagy in the *in vivo* process of vasculogenesis triggered by p17. It is worth noting that ET-1, unlike from p17, promotes neovessel formation in Beclin-1 knockout mice. This finding shows that different mechanisms than autophagy are activated by ET-1 and support its vasculogenic activity.

More recently, proviral sequences for p17 variants that display B-cell growth-promoting activity have been detected in HIV-NHL tissues, suggesting a role for p17 variants in lymphoma pathogenesis (35). Our data showing that a B-cell clonogenic p17 variant (NHL-a105) also displays lymphangiogenic activity through activation of autophagy makes it possible to formulate the hypothesis that these variants, because of their peculiar biologic properties on both B cells and ECs, are the most favorable

microenvironmental proteins to promote lymphoma development and spreading in HIV$^+$ patients. This hypothesis needs to be sustained by the development of evidence that B-cell clonogenic p17 variants are expressed in blood and in the lymph node microenvironment, as fully demonstrated for p17 (10–12). Interestingly, a recent study further supports the lymphomagenic ability of p17 since it shows that the expression of the viral protein in lymphoid tissues and bone marrow of HIV-1 transgenic mice carrying a noninfectious provirus is associated with B-cell lymphoma development (41). Collectively, all this evidence corroborates the hypothesis that p17 and its variant proteins may play a key role in producing a microenvironment that fosters lymphoma growth and metastasis.

Lymphomas originate in and spread along the lymphatic system. Up until now, there has been a lack of specific inhibitors of lymphangiogenesis. Most of the approved clinical trials rely on the use of drugs targeting the vascular endothelial growth factor C/D (VEGF-C/D) receptor 3 axis, a vessel-targeting therapy aimed to inhibit new vessel formation and to destroy the tumor vasculature (42). However, clinical trial results so far have been disappointing, and some reports even documented increased invasiveness and metastasis of the tumor after vessel-targeting therapy (43, 44). Our data suggest a novel strategy to inhibit ARL development and metastasis by directly targeting p17 and its B-cell growth-promoting variants. This may be achieved by using a specific therapeutic vaccine aimed to generate a neutralizing p17 response (45) or by using p17-specific drugs (46). There is increasing interest in the role that autophagic dysregulation may play in different vascular pathologies (21). Although we are far from developing pharmacologic modulators of autophagy, advancements in our understanding of the specific pathways used to extracellularly deliver bioactive molecules have motivated research attempts to develop small-molecule modulators of autophagy (47). The new knowledge gained from our study, showing that blocking autophagy and autophagy-based secretory pathways by pharmacological and genetic tools impairs the detrimental lymphangiogenic activity of both p17 and its B-cell clonogenic variant, opens the way to identify novel and exploitable targets for treating and/or preventing lymphoma development and metastasis. More importantly, our findings reveal a previously unrecognized role of autophagy in lymphangiogenesis. Since different types of carcinoma are able to induce lymphangiogenesis and use the lymphatic route to metastasize, this new knowledge calls for more general studies aimed at exploring the role of autophagy in driving aberrant tumor lymphangiogenesis.

MATERIALS AND METHODS

Recombinant proteins and MAb to p17. Purified endotoxin (lipopolysaccharide)-free recombinant p17 (from clone BH10 of clade B isolate), NHL-a105 (a B-cell clonogenic p17 variant derived from an HIV$^+$ patient with NHL) (35), glutathione *S*-transferase (GST), and the HIV-1 capsid protein p24 (p24) were produced as previously described (14, 35, 48). The absence of endotoxin contamination (<0.25 endotoxin units/ml) in protein preparations was assessed by the *Limulus* amebocyte assay (Associates of Cape Cod, Inc.). The p17 neutralizing monoclonal antibody (MAb) MBS-3 (48) was produced in our laboratory.

Human LN-LECs. LN-LECs have been previously developed and characterized (49). Cells were cultured in endothelial growth medium (EGM) (Lonza) containing 10% fetal bovine serum (FBS) and supplemented with VEGF-C (25 ng/ml; Reliatech). All experiments were carried out with cells at passages 2 to 6.

siRNA technique. Nucleoporation of LN-LECs was performed using the Amaxa Nucleofector Technology (Lonza). Small interfering RNAs (siRNAs) at 300 nM were added to 1×10^6 cells resuspended in 100 μl of nucleofection buffer. Silencing was carried out using a Beclin-1 siRNA (Cell Signaling Technology) and four distinct siRNAs targeting four different regions of the Rab8a and GRASP55 proteins (Dharmacon). Irrelevant siRNAs (siScramble; Cell Signaling Technology) were used as a negative control. The efficacy of silencing was evaluated by Western blotting.

Western blot analysis. LN-LECs (1×10^6) were nucleofected with siRNAs specific for Beclin-1, Rab8a, or GRASP55 or with siScramble. Twenty-four hours after nucleofection, cells were lysed in 200 μl of lysis buffer (10 mM HEPES [pH 7.9], 10 mM KCl, 1.5 mM $MgCl_2$, 0.5 mM EGTA, 0.5 mM EDTA, 0.6% Nonidet P-40 [Sigma-Aldrich]) containing a mixture of protease inhibitors (Complete Mini; Roche) and phosphatase inhibitors (1 mM sodium orthovanadate, 20 μM phenylarsine oxide [PAO], and 30 mM sodium fluoride [Sigma-Aldrich]). Equal amounts of total proteins were resolved on a 12% SDS-polyacrylamide gel and then electroblotted onto a nitrocellulose membrane. The blots were incubated overnight at 4°C with an MAb to Beclin-1 (Cell Signaling Technology), polyclonal antibody (pAb) to GRASP55 (ProteinTech Group), MAb to Rab8a (Abcam), and MAb to glyceraldehyde-3-phosphate dehydrogenase (GAPDH) (Santa Cruz

Biotechnology). The antigen-antibody complex was detected by incubation of the membranes for 1 h at room temperature with peroxidase-conjugated goat polyclonal antibody to rabbit IgG or goat polyclonal antibody to mouse IgG (Thermo Scientific) and revealed using Clarity Western ECL substrate (Bio-Rad). Images were acquired by a ChemiDoc-it System (Bio-Rad), and protein expression was determined using Gel-Pro Analyzer software (Media Cybernetics).

***In vitro* tube formation assay.** LN-LECs were grown under normal (10% FBS) or stressed (serum-starved; 0.5% FBS) conditions for 16 h in endothelial basal medium (EBM) and then harvested and resuspended in EGM containing 10% FBS. Cells were seeded (5×10^4 cells per well) in wells coated with growth factor-reduced Cultrex basement membrane extract (BME; Trevigen) and left untreated or treated for 12 h with different concentrations (ranging from 10 to 500 ng/ml) of GST, p24, or p17 or with 10 ng/ml of NHL-a105. When indicated on the figures, cells were nucleofected with siRNAs specific for Beclin-1, Rab8a, or GRASP55 or with siScramble. In some experiments, LN-LECs were pretreated for 16 h at 37°C with 5 mM 3-methyladenine (3-MA) (Sigma-Aldrich) and with different concentrations, ranging from 1 to 50 μM, of CA-074Me, a pharmacologic inhibitor of cathepsin-β (Enzo Life Science). When reported on the figures, p17 was preincubated for 30 min at 37°C with 1 μg/ml of unrelated control MAb (Ctrl MAb) or p17 neutralizing MAb MBS-3. In selected experiments, starved LN-LECs were pretreated with 2.5 μg/ml of MAb to CXCR1 (MAb 330; R&D) and CXCR2 (MAb 331; R&D) alone or in combination (1.25 μg/ml each) or with an isotype-matched MAb (2.5 μg/ml; R&D) for 1 h at 37°C before p17 stimulation. Wells were then analyzed for the formation of tube structures.

Autophagy fluorescence assay. LN-LECs were nucleofected with an EGFP-LC3-expressing plasmid (EGFP-LC3; plasmid 11546 [Addgene]). Twenty-four hours after nucleofection, cells were plated on collagen-coated glass coverslips and then starved for 16 h in EBM–0.5% FBS alone or in combination with 3-MA (5 mM). Cells were left untreated or treated for 3 h with 10 ng/ml of GST, p24, or p17 and fixed with 4% paraformaldehyde. When reported on the figures, p17 was preincubated for 30 min at 37°C with 1 μg/ml of unrelated control MAb (Ctrl MAb) or p17 neutralizing MAb MBS-3. In selected experiments, starved LN-LECs were pretreated with 2.5 μg/ml of MAb to CXCR1 and CXCR2 alone or in combination (1.25 μg/ml each) or with an isotype-matched MAb (2.5 μg/ml) for 1 h at 37°C before p17 stimulation. Fluorescence was analyzed using a Leica TCS SP5 laser scanning fluorescence microscope and the imaging software Leica Application Suite.

Wound-healing assay. LN-LECs were plated on 24-well plates (1×10^5 cells per well) in EGM containing 10% FBS and VEGF-C (25 ng/ml). Confluent monolayers were nutrient starved for 16 h in the presence or absence of 3-MA (5 mM) and then scratched using a 200-μl pipette tip. After being washed, cells were left untreated or treated with 10 ng/ml of GST, p24, or p17.

Human ET-1 quantitative ELISA. Subconfluent LN-LECs were starved for 16 h alone or in combination with 3-MA (5 mM) and cultured for 1, 3, and 6 h in the presence of 10 ng/ml of GST, p24, p17, or NHL-a105. Samples of the conditioned medium were then collected at 1, 3, and 6 h after the beginning of culture and stored in aliquots at −80°C. ET-1 expression was measured by ELISA (Enzo Life Science). In some experiments, LN-LECs were nucleofected with siScramble, siGRASP55, or siRab8a, and 24 h after nucleofection, cells were serum starved for 16 h and then stimulated with 10 ng/ml of GST, p24, p17, and NHL-a105. When reported on the figures, LN-LECs were serum starved for 16 h in the presence or absence of 3-MA (5 mM) or CA-074Me (50 μM).

***In vivo* lymphangiogenesis assay.** Lymphangiogenesis was evaluated *in vivo* using a Matrigel plug assay as previously described (17). Female C57BL/6 and B6.129X1 Becn^{1tm1Blev} mice carrying a monoallelic deletion of the autophagy-related Beclin-1 gene (BECN-1 KO) were purchased from The Jackson Laboratory. Mice (age, 6 to 8 weeks; 5 per group) were handled according to the local government of Lower Saxony, Germany (approval number 33.9-42502-04-11/0368). Mice were injected subcutaneously with 500 μl of growth factor-reduced Cultrex BME (Trevigen). Gel implants were supplemented with 200 ng/ml of p17, 200 ng/ml of ET-1 (R&D Systems), or PBS. Ten days postinjection, the gel implants were removed from the mice, fixed, and paraffin embedded.

Immunohistochemistry. Paraffin sections were deparaffinized in xylene and rehydrated in a graded ethanol series. For antigen retrieval, slides were placed in a pressure cooker in citrate buffer (pH 7.6). Endogenous peroxidase was blocked with 3% H_2O_2. Subsequently, slides were blocked with ready-to-use blocking solution (Zytomed Systems). CD31 (cluster of differentiation 31) was detected using a rat anti-mouse CD31 monoclonal antibody (MAb) (Dianova) diluted in antibody diluent (Zytomed Systems) as a primary antibody. As secondary antibody, biotinylated goat anti-rat (Kirkegaard & Perry Labs) was applied. Subsequently, streptavidin-horseradish peroxidase (HRP) conjugate (Zytomed Systems), 3-3′-diaminobenzidine-tetrahydrochloride (DAB) chromogen, and substrate buffer (Zytomed Systems) were added. Counterstaining was performed with hematoxylin (Merck Millipore). The slides were randomized and blinded as to the experimental groups and analyzed using a light microscope (Zeiss AxioScope).

Statistical analysis. Data obtained from multiple independent experiments are expressed as the means ± the standard deviations (SDs). The data were analyzed for statistical significance using one-way analysis of variance (ANOVA). Bonferroni's posttest was used to compare data. Differences were considered significant at a P value of <0.05. Statistical tests were performed using Prism 5 software (GraphPad).

ACKNOWLEDGMENTS

We thank Giuseppe Crea for his skillful technical assistance and Blair Prochnow and Ingo Schmitz for critical readings of the manuscript.

REFERENCES

1. Engsig FN, Zangerle R, Katsarou O, Dabis F, Reiss P, Gill J, Porter K, Sabin C, Riordan A, Fätkenheuer G, Gutiérrez F, Raffi F, Kirk O, Mary-Krause M, Stephan C, de Olalla PG, Guest J, Samji H, Castagna A, d'Arminio Monforte A, Skaletz-Rorowski A, Ramos J, Lapadula G, Mussini C, Force L, Meyer L, Lampe F, Boufassa F, Bucher HC, De Wit S, Burkholder GA, Teira R, Justice AC, Sterling TR, Crane MH, Gerstoft J, Grarup J, May M, Chêne G, Ingle SM, Sterne J, Obel N, Antiretroviral Therapy Cohort Collaboration (ART-CC), the Collaboration of Observational HIV Epidemiological Research Europe (COHERE) in EuroCoord. 2014. Long-term mortality in HIV-positive individuals virally suppressed for >3 years with incomplete CD4 recovery. Clin Infect Dis 58:1312–1321. https://doi.org/10.1093/cid/ciu038.
2. McManus H, O'Connor CC, Boyd M, Broom J, Russell D, Watson K, Roth N, Read PJ, Petoumenos K, Law MG, Australian HIV Observational Database. 2012. Long-term survival in HIV positive patients with up to 15 years of antiretroviral therapy. PLoS One 7:e48839. https://doi.org/10.1371/journal.pone.0048839.
3. Rubinstein PG, Aboulafia DM, Zloza A. 2014. Malignancies in HIV/AIDS: from epidemiology to therapeutic challenges. AIDS 28:453–465. https://doi.org/10.1097/QAD.0000000000000071.
4. Borges ÁH. 2017. Combination antiretroviral therapy and cancer risk. Curr Opin HIV AIDS 12:12–19. https://doi.org/10.1097/COH.0000000000000334.
5. Shepherd L, Borges ´A, Ledergerber B, Domingo P, Castagna A, Rockstroh J, Knysz B, Tomazic J, Karpov I, Kirk O, Lundgren J, Mocroft A, EuroSIDA in EuroCOORD. 2016. Infection-related and -unrelated malignancies, HIV and the aging population. HIV Med 17:590–600. https://doi.org/10.1111/hiv.12359.
6. Pepper MS, Tille JC, Nisato R, Skobe M. 2003. Lymphangiogenesis and tumor metastasis. Cell Tissue Res 314:167–177. https://doi.org/10.1007/s00441-003-0748-7.
7. Taylor JG, Liapis K, Gribben JG. 2015. The role of the tumor microenvironment in HIV-associated lymphomas. Biomark Med 9:473–482. https://doi.org/10.2217/bmm.15.13.
8. Mazzuca P, Caruso A, Caccuri F. 2016. HIV-1 infection, microenvironment and endothelial cell dysfunction. New Microbiol 39:163–173.
9. Wiley EL, Nightingale SD. 1994. Opportunistic events and p17 expression in the bone marrow of human immunodeficiency virus-infected patients. J Infect Dis 169:617–620. https://doi.org/10.1093/infdis/169.3.617.
10. Fiorentini S, Riboldi E, Facchetti F, Avolio M, Fabbri M, Tosti G, Becker PD, Guzman CA, Sozzani S, Caruso A. 2008. HIV-1 matrix protein p17 induces human plasmacytoid dendritic cells to acquire a migratory immature cell phenotype. Proc Natl Acad Sci U S A 105:3867–3872. https://doi.org/10.1073/pnas.0800370105.
11. Popovic M, Tenner-Racz K, Pelser C, Stellbrink HJ, van Lunzen J, Lewis G, Kalyaraman VS, Gallo RC, Racz P. 2005. Persistence of HIV-1 structural proteins and glycoproteins in lymph nodes of patients under highly active antiretroviral therapy. Proc Natl Acad Sci U S A 102:14807–14812. https://doi.org/10.1073/pnas.0506857102.
12. Dolcetti R, Gloghini A, Caruso A, Carbone A. 2016. A lymphomagenic role for HIV beyond immune suppression? Blood 127:1403–1409. https://doi.org/10.1182/blood-2015-11-681411.
13. Pace MJ, Graf EH, Agosto LM, Mexas AM, Male F, Brady T, Bushman FD, O'Doherty U. 2012. Directly infected resting $CD4^+$ T cells can produce HIV Gag without spreading infection in a model of HIV latency. PLoS Pathog 8:e1002818. https://doi.org/10.1371/journal.ppat.1002818.
14. Caccuri F, Ilaria ML, Campilongo F, Varney K, Rossi A, Mitola S, Schiarea S, Bugatti A, Mazzuca P, Giagulli C, Fiorentini S, Lu W, Salmona M, Caruso A. 2016. Cellular aspartyl proteases promote the unconventional secretion of biologically active HIV-1 matrix protein p17. Sci Rep 6:38027. https://doi.org/10.1038/srep38027.
15. Fiorentini S, Marini E, Caracciolo S, Caruso A. 2006. Functions of the HIV-1 matrix protein p17. New Microbiol 29:1–10.
16. Caccuri F, Giagulli C, Bugatti A, Benetti A, Alessandri G, Ribatti D, Marsico S, Apostoli P, Slevin MA, Rusnati M, Guzman CA, Fiorentini S, Caruso A. 2012. HIV-1 matrix protein p17 promotes angiogenesis via chemokine receptors CXCR1 and CXCR2. Proc Natl Acad Sci U S A 109:14580–14585. https://doi.org/10.1073/pnas.1206605109.
17. Caccuri F, Rueckert C, Giagulli C, Schulze K, Basta D, Zicari S, Marsico S, Cervi E, Fiorentini S, Slevin M, Guzman CA, Caruso A. 2014. HIV-1 matrix protein p17 promotes lymphangiogenesis and activates the endothelin-1/endothelin B receptor axis. Arterioscler Thromb Vasc Biol 34:846–856. https://doi.org/10.1161/ATVBAHA.113.302478.
18. Caccuri F, Marsico S, Fiorentini S, Caruso A, Giagulli C. 2016. HIV-1 matrix protein p17 and its receptors. Curr Drug Targets 17:23–32. https://doi.org/10.2174/1389450116666150825110840.
19. Glick D, Barth S, Macleod KF. 2010. Autophagy: cellular and molecular mechanisms. J Pathol 221:3–12. https://doi.org/10.1002/path.2697.
20. Du J, Teng RJ, Guan T, Eis A, Kaul S, Konduri GG, Shi Y. 2012. Role of autophagy in angiogenesis in aortic endothelial cells. Am J Physiol Cell Physiol 302:C383–C391. https://doi.org/10.1152/ajpcell.00164.2011.
21. Nussenzweig SC, Verma S, Finkel T. 2015. The role of autophagy in vascular biology. Circ Res 116:480–488. https://doi.org/10.1161/CIRCRESAHA.116.303805.
22. Wu YT, Tan HL, Shui G, Bauvy C, Huang Q, Wenk MR, Ong CN, Codogno P, Shen HM. 2010. Dual role of 3-methyladenine in modulation of autophagy via different temporal patterns of inhibition on class I and III phosphoinositide 3-kinase. J Biol Chem 285:10850–10861. https://doi.org/10.1074/jbc.M109.080796.
23. Tanida I, Ueno T, Kominami E. 2008. LC3 and autophagy. Methods Mol Biol 445:77–88. https://doi.org/10.1007/978-1-59745-157-4_4.
24. Mizushima N, Yoshimori T, Levine B. 2010. Methods in mammalian autophagy research. Cell 140:313–326. https://doi.org/10.1016/j.cell.2010.01.028.
25. Ueno T, Sato W, Horie Y, Komatsu M, Tanida I, Yoshida M, Ohshima S, Mak TW, Watanabe S, Kominami E. 2008. Loss of Pten, a tumor suppressor, causes the strong inhibition of autophagy without affecting LC3 lipidation. Autophagy 4:692–700. https://doi.org/10.4161/auto.6085.
26. Liang XH, Jackson S, Seaman M, Brown K, Kempkes B, Hibshoosh H, Levine B. 1999. Induction of autophagy and inhibition of tumorigenesis by beclin 1. Nature 402:672–676. https://doi.org/10.1038/45257.
27. Tassa A, Roux MP, Attaix D, Bechet DM. 2003. Class III phosphoinositide 3-kinase–Beclin1 complex mediates the amino acid-dependent regulation of autophagy in C2C12 myotubes. Biochem J 376:577–586. https://doi.org/10.1042/bj20030826.
28. Zeng X, Overmeyer JH, Maltese WA. 2006. Functional specificity of the mammalian Beclin-Vps34 PI 3-kinase complex in macroautophagy versus endocytosis and lysosomal enzyme trafficking. J Cell Sci 119:259–270. https://doi.org/10.1242/jcs.02735.
29. Mo J, Zhang D, Yang R. 2016. MicroRNA-195 regulates proliferation, migration, angiogenesis and autophagy of endothelial progenitor cells by targeting GABARAPL1. Biosci Rep 36:e00396. https://doi.org/10.1042/BSR20160139.
30. Duran JM, Anjard C, Stefan C, Loomis WF, Malhotra V. 2010. Unconventional secretion of Acb1 is mediated by autophagosomes. J Cell Biol 188:527–536. https://doi.org/10.1083/jcb.200911154.
31. Manjithaya R, Anjard C, Loomis WF, Subramani S. 2010. Unconventional secretion of Pichia pastoris Acb1 is dependent on GRASP protein, peroxisomal functions, and autophagosome formation. J Cell Biol 188:537–546. https://doi.org/10.1083/jcb.200911149.
32. Dupont N, Jiang S, Pilli M, Ornatowski W, Bhattacharya D, Deretic V. 2011. Autophagy-based unconventional secretory pathway for extracellular delivery of IL-1β. EMBO J 30:4701–4711. https://doi.org/10.1038/emboj.2011.398.
33. Bodemann BO, Orvedahl A, Cheng T, Ram RR, Ou YH, Formstecher E, Maiti M, Hazelett CC, Wauson EM, Balakireva M, Camonis JH, Yeaman C, Levine B, White MA. 2011. RalB and the exocyst mediate the cellular starvation response by direct activation of autophagosome assembly. Cell 144:253–267. https://doi.org/10.1016/j.cell.2010.12.018.
34. Basta D, Latinovic O, Lafferty MK, Sun L, Bryant J, Lu W, Caccuri F, Caruso A, Gallo R, Garzino-Demo A. 2015. Angiogenic, lymphangiogenic and adipogenic effects of HIV-1 matrix protein p17. Pathog Dis 73:ftv062. https://doi.org/10.1093/femspd/ftv062.
35. Dolcetti R, Giagulli C, He W, Selleri M, Caccuri F, Eyzaguirre LM, Mazzuca P, Corbellini S, Campilongo F, Marsico S, Giombini E, Muraro E, Rozera G, De Paoli P, Carbone A, Capobianchi MR, Ippolito G, Fiorentini S, Blattner WA, Lu W, Gallo RC, Caruso A. 2015. Role of HIV-1 matrix protein p17 variants in lymphoma pathogenesis. Proc Natl Acad Sci U S A 112:14331–14336. https://doi.org/10.1073/pnas.1514748112.
36. Caccuri F, Giagulli C, Reichelt J, Martorelli D, Marsico S, Bugatti A, Barone I, Rusnati M, Guzman CA, Dolcetti R, Caruso A. 2014. Simian immunodeficiency virus and human immunodeficiency virus type 1 matrix pro-

teins specify different capabilities to modulate B cell growth. J Virol 88:5706–5717. https://doi.org/10.1128/JVI.03142-13.
37. Rabkin CS. 2001. AIDS and cancer in the era of highly active antiretroviral therapy (HAART). Eur J Cancer 37:1316–1319. https://doi.org/10.1016/S0959-8049(01)00104-6.
38. Knowles DM, Pirog EC. 2001. Pathology of AIDS-related lymphomas and other AIDS-defining neoplasms. Eur J Cancer 37:1236–1250. https://doi.org/10.1016/S0959-8049(01)00103-4.
39. Baumgartner JE, Rachlin JR, Beckstead JH, Meeker TC, Levy RM, Wara WM, Rosenblum ML. 1990. Primary central nervous system lymphomas: natural history and response to radiation therapy in 55 patients with acquired immunodeficiency syndrome. J Neurosurg 73:206–211. https://doi.org/10.3171/jns.1990.73.2.0206.
40. Lerner TR, de Souza Carvalho-Wodarz C, Repnik U, Russell MR, Borel S, Diedrich CR, Rohde M, Wainwright H, Collinson LM, Wilkinson RJ, Griffiths G, Gutierrez MG. 2016. Lymphatic endothelial cells are a replicative niche for *Mycobacterium tuberculosis*. J Clin Invest 126:1093–1108. https://doi.org/10.1172/JCI83379.
41. Carroll VA, Lafferty MK, Marchionni L, Bryant JL, Gallo RC, Garzino-Demo A. 2016. Expression of HIV-1 matrix protein p17 and association with B-cell lymphoma in HIV-1 transgenic mice. Proc Natl Acad Sci U S A 113:13168–13173. https://doi.org/10.1073/pnas.1615258113.
42. Potente M, Gerhardt H, Carmeliet P. 2011. Basic and therapeutic aspects of angiogenesis. Cell 146:873–887. https://doi.org/10.1016/j.cell.2011.08.039.
43. Welti J, Loges S, Dimmeler S, Carmeliet P. 2013. Recent molecular discoveries in angiogenesis and antiangiogenic therapies in cancer. J Clin Invest 123:3190–3200. https://doi.org/10.1172/JCI70212.
44. Huang Y, Stylianopoulos T, Duda DG, Fukumura D, Jain RK. 2013. Benefits of vascular normalization are dose and time dependent–letter. Cancer Res 73:7144–7146. https://doi.org/10.1158/0008-5472.CAN-13-1989.
45. Iaria ML, Fiorentini S, Focà E, Zicari S, Giagulli C, Caccuri F, Francisci D, Di Perri G, Castelli F, Baldelli F, Caruso A. 2014. Synthetic HIV-1 matrix protein p17-based AT20-KLH therapeutic immunization in HIV-1-infected patients receiving antiretroviral treatment: a phase I safety and immunogenicity study. Vaccine 32:1072–1078. https://doi.org/10.1016/j.vaccine.2013.12.051.
46. Haffar O, Dubrovsky L, Lowe R, Berro R, Kashanchi F, Godden J, Vanpouille C, Bajorath J, Bukrinsky M. 2005. Oxadiazols: a new class of rationally designed anti-human immunodeficiency virus compounds targeting the nuclear localization signal of the viral matrix protein. J Virol 79:13028–13036. https://doi.org/10.1128/JVI.79.20.13028-13036.2005.
47. Vakifahmetoglu-Norberg H, Xia HG, Yuan J. 2015. Pharmacologic agents targeting autophagy. J Clin Invest 125:5–13. https://doi.org/10.1172/JCI73937.
48. De Francesco MA, Baronio M, Fiorentini S, Signorini C, Bonfanti C, Poiesi C, Popovic M, Grassi M, Garrafa E, Bozzo L, Lewis GK, Licenziati S, Gallo RC, Caruso A. 2002. HIV-1 matrix protein p17 increases the production of proinflammatory cytokines and counteracts IL-4 activity by binding to a cellular receptor. Proc Natl Acad Sci U S A 99:9972–9977. https://doi.org/10.1073/pnas.142274699.
49. Norder M, Gutierrez MG, Zicari S, Cervi E, Caruso A, Guzmán CA. 2012. Lymph node-derived lymphatic endothelial cells express functional costimulatory molecules and impair dendritic cell-induced allogenic T-cell proliferation. FASEB J 26:2835–2846. https://doi.org/10.1096/fj.12-205278.